

Controlling surface morphologies by time-delayed feedback

M. Block,^{1,*} B. Schmittmann,² and E. Schöell¹

¹*Institut für Theoretische Physik, Technische Universität Berlin, D-10623 Berlin, Germany*

²*Department of Physics, Virginia Tech, Blacksburg, Virginia 24061, USA*

(Received 2 May 2007; published 25 June 2007)

We propose a method to control the roughness of a growing surface via a time-delayed feedback scheme. The method is very general and can be applied to a wide range of nonequilibrium growth phenomena, from solid-state epitaxy to tumor growth. Possible experimental realizations are suggested. As an illustration, we consider the Kardar-Parisi-Zhang equation [Phys. Rev. Lett. **56**, 889 (1986)] in 1+1 dimensions and show that the effective growth exponent of the surface width can be stabilized at any desired value in the interval [0.25, 0.33], for a significant length of time.

DOI: [10.1103/PhysRevB.75.233414](https://doi.org/10.1103/PhysRevB.75.233414)

PACS number(s): 68.35.Rh, 05.10.Gg, 02.30.Ks, 02.60.Cb

The control of unstable states in chaotic or pattern-forming nonlinear dynamical systems has attracted much interest recently.^{1,2} Time-delayed feedback control³ has been especially successful in stabilizing a variety of dynamic and spatial structures, including noise-induced oscillations and patterns found, e.g., in semiconductor nanostructures.^{4–7} Here, we propose to apply these control techniques to a completely new class of dynamical phenomena, namely, far-from-equilibrium surface growth.^{8–10} The goal is to stabilize desired surface characteristics, such as spatiotemporal height-height correlations or the surface roughness, during the growth process. Even if such control can only be sustained in a finite window of time, its experimental potential is undiminished since the growth process can simply be terminated when the desired characteristics have been achieved, thanks to today's precise *in situ* characterization capabilities. Moreover, paradigmatic growth models, such as the Kardar-Parisi-Zhang (KPZ) equation,¹¹ find applications in many diverse areas of science, e.g., thin film growth,^{12–15} fluctuating hydrodynamics,¹⁶ driven diffusive systems,^{17–19} tumor growth in biophysics,^{20–22} propagating fire fronts,²³ and econophysics.²⁴ Therefore, broad implications can be expected if methods from control theory can be successfully implemented in this vast context.

In this Brief Report, we provide an exploration of these ideas. We choose the most promising type of control, time-delayed feedback, and study its effects on the KPZ equation.¹¹ Specifically, we attempt to control the *effective* dynamic growth exponent β associated with the roughness of the growing surface. By implementing two realizations of the control scheme, we will see below that we can, indeed, stabilize β in a range of values between the two universal limits, 1/4 and 1/3, over at least one to two decades in time. In the following, we will use the language of surface growth, but our findings are just as relevant in the context of all other applications of the KPZ equation. For instance, in recent work on tumor growth,²⁰ it has been shown that an efficient method to influence the proliferation of tumor cells at the border is coupled to the growth exponents and the universal class of growth. The authors suggest and establish a therapy which rests on the possibility of tunable roughness.

The fabrication of nanostructures typically involves the deposition of a material onto a substrate. One of the primary experimental goals is to achieve nanoscale control of layer

thickness and surface morphology. For many thin film applications, for instance, in optics²⁵ or in semiconductor nanostructures, it is essential to control and adjust the roughness, e.g., in order to minimize scattering losses. On the theoretical side, considerable effort has been focused on developing suitable evolution equations for the growing layer.¹⁰ While many different versions^{8,9,26–31} of such equations exist, depending on the details of deposition processes and molecular interactions and kinetics, all of them share certain fundamental characteristics: they are noisy, nonlinear partial differential equations in space and time, and describe an important class of generic nonequilibrium phenomena.

If overhangs and bulk fluctuations can be neglected, a single-valued variable, $h(x, t)$, suffices to denote the height of the surface above a reference plane and fluctuates as a function of time t and position x (measured in this d -dimensional plane). The simplest such equation is the KPZ equation,¹¹ which describes the growth of a surface in the absence of any conservation laws:

$$\partial_t h(x, t) = \nu \nabla^2 h(x, t) + \frac{\lambda}{2} (\nabla h)^2 + \eta(x, t). \quad (1)$$

Here, $\nu > 0$ denotes an interface smoothing term, associated with a surface tension; the nonlinear coupling λ reflects the strength of lateral growth, and $\eta(x, t)$ models the height fluctuations due to random deposition of material. An overall, constant growth velocity has already been eliminated by transforming into a suitable comoving frame. Focusing on large-scale, long-time properties of the surface, it is sufficient to consider Gaussian white noise, i.e., $\langle \eta(x, t) \rangle = 0$, $\langle \eta(x, t) \eta(x', t') \rangle = 2D \delta^d(x - x') \delta(t - t')$. For simplicity, we restrict ourselves to one spatial dimension. We monitor the time dependence of the (root mean square) surface roughness w , defined by

$$w^2(L, t) = \frac{1}{L} \left\langle \sum_x [h(x, t) - \bar{h}(t)]^2 \right\rangle. \quad (2)$$

Here, L denotes the system size, and $\bar{h}(t) \equiv L^{-1} \sum_x h(x, t)$ is the mean surface height at time t . Configurational averages are denoted by $\langle \cdots \rangle$. The sum over x anticipates the space discretization associated with the numerical integration scheme.

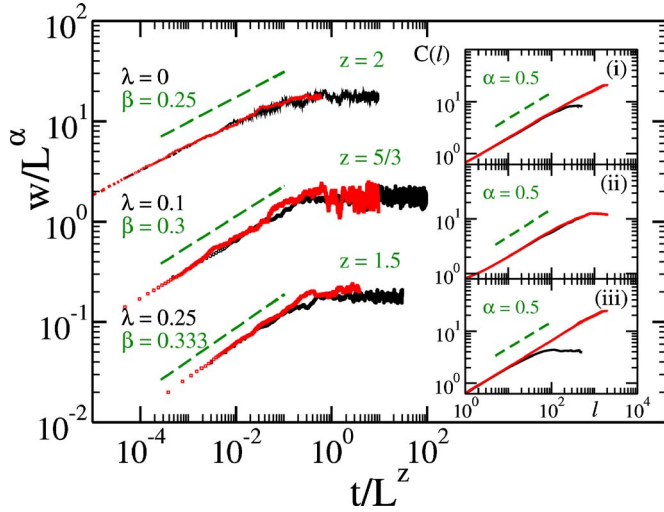


FIG. 1. (Color online) Scaling plots of the roughness $w(L, t)$ and height-height correlation function $C(l) \equiv \langle h(l, t)h(0, t) \rangle \sim l^\alpha$ (insets) for system sizes $L=1024$ (red/light gray) and $L=4096$ (black) and three choices of λ : (i) $\lambda=0$ (shifted by a factor 100), (ii) $\lambda=0.1$ (shifted by a factor 10), and (iii) $\lambda=0.25$. $\nu=0.1$, $D=0.5$ for all data sets; space discretization $\Delta x=1$ and time increment $\Delta t=10^{-3}$. The green broken lines provide guides for the eyes.

It is well known that w obeys scaling in the form $w(L, t) = L^\alpha f(t/L^z)$, where f is a scaling function, and α and z denote the roughness and dynamic exponents, respectively.³² In the saturation regime ($t/L^z \gg 1$) $w \sim L^\alpha$, whereas in the growth regime ($t/L^z \ll 1$) $w \sim t^\beta$, with a growth exponent β . Consistency with the general scaling form imposes an exponent identity, $\beta = \alpha/z$. Two universality classes can be distinguished: If the nonlinear term of the KPZ equation vanishes ($\lambda=0$), the equation reduces to the exactly soluble Edwards-Wilkinson (EW) equation,³³ with $\alpha=1/2$ and $z=2$, whence $\beta=1/4$. In contrast, any *nonzero* value of λ belongs to the KPZ universality class, with $\alpha=1/2$ and $z=3/2$, whence $\beta=1/3$.¹¹ These values give us some benchmarks against which we can check our numerical scheme. We use a forward-backward Euler method^{34,35} to solve numerically the stochastic differential equations. λ varies between 0.00 and 0.25. The upper cutoff is chosen so as to avoid numerical instabilities. Figure 1 shows a scaling plot for $w(L, t)$ before any control schemes are implemented. Data for three different values of λ are shown. The roughness exponent α is consistent with $1/2$, independent of λ , as expected. For $\lambda=0$, we see excellent data collapse with the EW scaling exponents, and the KPZ exponents are confirmed for the largest λ . The latter should be universal, for all $\lambda \neq 0$; however, for $0 < \lambda < 0.25$, strong crossover effects between EW and KPZ behaviors are observed. Remarkably, this crossover manifests itself as a surprisingly clean power law, with a λ -dependent effective growth exponent β below $1/3$. Eventually, the asymptotic value ($1/3$) is reached, but only after an L - and λ -dependent crossover time.

We now turn to possible control mechanisms. For chemical vapor deposition of silica films, there is some experimental evidence¹² that the lateral growth velocity is related to the temperature, via a temperature-dependent sticking probabil-

ity. In other words, λ —and hence effective growth exponents—can be controlled via the temperature. For our differential equation, we tune λ directly, in order to stabilize a *desired* effective growth exponent β_0 . In detail, the scheme is as follows. First, we choose the desired value of the growth exponent β_0 and select an appropriate time delay τ . Generating sufficiently many samples of $h(x, t)$, we record $w(t-\tau)$ and $w(t)$ (the argument L will be omitted from now on). The *local* exponent β_{local} at time t is defined as

$$\beta_{local}(t) \equiv \frac{\log w(t) - \log w(t-\tau)}{\log t - \log(t-\tau)}. \quad (3)$$

Depending on the sign and value of $\beta_{local}(t) - \beta_0$, we adjust the nonlinear coupling λ of the KPZ equation as follows. First, we introduce a control function $F(t)$. For *digital* control, we define

$$F(t) \equiv \begin{cases} a & \text{if } \beta_{local} \leq \beta_0 \\ -a & \text{if } \beta_{local} > \beta_0, \end{cases} \quad (4)$$

where the parameter a defines the control “bit,” i.e., the amount by which λ changes at each control step. Alternatively, we also investigate a *differential* method for which

$$F(t) \equiv K(\beta_0 - \beta_{local}), \quad (5)$$

and K sets the amplitude of the control strength. Given one of the two choices of $F(t)$, the control scheme sets in at time t_0 . From then on, the nonlinearity λ is updated at times $t_n \equiv t_0 + n\tau$, $n=1, 2, \dots$, starting from an initial value λ_0 , according to

$$\lambda(t) = \begin{cases} \lambda_0 & \text{if } t < t_0 \\ \lambda(t-\tau) + F(t) & \text{if } t = t_n \\ \lambda(t_n) & \text{if } t_n < t < t_{n+1}. \end{cases} \quad (6)$$

Our scheme is successful if $\beta_{local}(t)$ approaches β_0 and then settles at the desired value within a reasonable time frame after the control has been activated. Some comments are in order. Starting from a random initial condition, we first choose a starting value, λ_0 , for the nonlinearity and integrate the KPZ equation without control up to time t_0 in order to eliminate transients. A reasonably stable growth regime is achieved around $t_0 \sim 10$, independent of L (provided L is not too small, i.e., $L \geq 64$). Then, we turn on the control, following either the digital or the differential scenario. Regarding the choice of the time delay τ , it must be large enough compared to the time increment Δt so as not to interfere with the integration procedure, but small enough to provide responsive control. We find that we get good results for a time delay $0.1 < \tau < 1.0$. Similarly, we choose the control amplitudes a and K such that the increments in λ are small compared to λ_0 , but large enough to generate a noticeable response. For example, for $\tau=1.0$, choosing a in the range $[0.002, 0.02]$ and K in the range $[0.005, 0.05]$ provides the best results.

Figures 2 and 3 show our results. Starting from three initial values of λ_0 , namely, 0, 0.1, and 0.25, we attempt to stabilize the effective growth exponent at $\beta_0=0.29$, midway between the KPZ and EW values. Irrespective of λ_0 , we find that both digital and differential control result in an effective

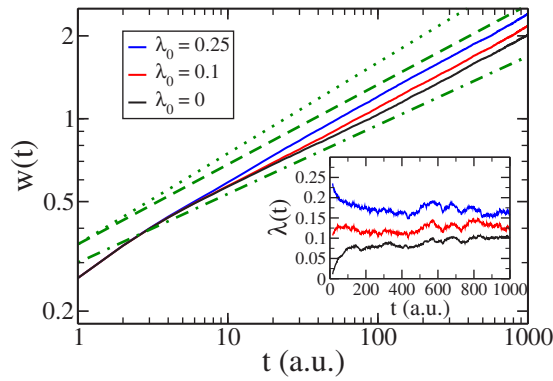


FIG. 2. (Color online) Roughness and control function (inset) evolution for digital time-delayed feedback control for strong (blue/dark gray), weak (red/light gray), and zero (black) initial nonlinearity λ_0 . The desired effective growth exponent is set at $\beta_0=0.29$. To provide a comparison, the straight (green) lines have slopes 0.33 (dotted), 0.29 (dashed), and 0.25 (dash-dotted). All data sets are obtained with $\nu=0.1$, $D=0.5$, and $a=0.01$.

growth exponent very close to the desired value, over at least a decade of integration time ($100 \leq t \leq 1000$). For sufficiently large time, the control function $\lambda(t)$ appears to approach a constant value, close to 0.15. However, the details of the approach depend on the initial λ_0 . For strong initial nonlinearity $\lambda_0=0.25$, $\lambda(t)$ is approximately monotonically decreasing, apart from significant fluctuations. For both weak and vanishing initial couplings, $\lambda(t)$ approaches its “limit” from below. This behavior is observed for both digital and differential control. We tested several other choices of $0.25 \leq \beta_0 < 0.33$ and λ_0 , and found similar behavior.

Experimentally, it is usually desirable to achieve small roughness. To push our control schemes to the limit, we test the most extreme case, namely, $\beta_0=0.25$ with large initial nonlinearity $\lambda_0=0.25$. Before the control sets in, the roughness grows considerably faster than $t^{0.25}$. As soon as the control sets in, $\lambda(t)$ decreases quite dramatically, leading to a

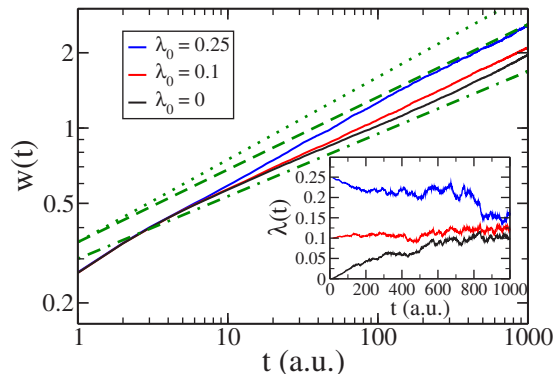


FIG. 3. (Color online) Roughness and control function (inset) evolution for differential time-delayed feedback control for strong (blue/dark gray), weak (red/light gray), and zero (black) initial nonlinearity λ_0 . The desired effective growth exponent is set at $\beta_0=0.29$. To provide a comparison, the straight (green) lines have slopes 0.33 (dotted), 0.29 (dashed), and 0.25 (dash-dotted). All data sets are obtained with $\nu=0.1$, $D=0.5$, and $K=0.02$.

reduction of the effective β . However, over the time period considered ($t \leq 1000$), it never decreases far enough to reach the desired 0.25.

Finally, we note that it is not possible to achieve exponent values *outside* the interval $[0.25, 0.33]$. Choosing $\beta_0 > 0.33$ generates unbounded growth of the control function $\lambda(t)$, accompanied by instabilities in the integration routine. Similarly, $\beta_0 < 0.25$ quickly leads to large *negative* values of $\lambda(t)$, which tend to favor KPZ exponents (since the sign of λ plays no role). As a result, $\lambda(t)$ becomes even more negative until a numerical instability occurs. To avoid this instability, we also implemented a symmetrized version of control [with $a \rightarrow -a$ when $\lambda(t) < 0$]. In this case, $\lambda(t)$ approaches zero and fluctuates about it, so that the effective exponent settles at 0.25.

To summarize, both digital and differential control are quite successful at stabilizing effective growth exponents in the KPZ equation. For the relatively small system sizes used here, these exponents can be tuned in the range $[0.25, 0.33]$, i.e., within the limits set by the EW and KPZ equations, respectively. Let us emphasize again that only the values $1/4$ (for $\lambda=0$) and $1/3$ (for any $\lambda \neq 0$) correspond to true asymptotic exponents; for larger system sizes and longer integration times, these emerge clearly. However, for small systems, we observe surprisingly clean effective growth exponents which appear to depend monotonically on the magnitude of the nonlinearity. Hence, it is possible to choose a desired reference exponent β_0 and implement a time-delayed control of the nonlinearity in such a way that the effective exponent first approaches β_0 and then stabilizes at that value for a significant length of time (roughly $10^2 \leq t \leq 10^3$ in our units). In all simulations, the (stationary) roughness remains constant at $\alpha=0.5$, reflecting the value $1/2$, which is common to both the EW and KPZ equations. The control protocol itself is independent of the dimension of the surface. Work is in progress to test other growth equations and to extend the KPZ study to 2+1 dimensions. For the experimental implementation and feasibility of our method in epitaxial growth, it should be noted that recent achievements of *in situ* scanning tunneling microscopy during real-time growth^{36–38} open up the possibility to measure the time-dependent roughness and use it for temperature control in a feedback loop during the growth process. In the paradigmatic KPZ equation, which contains only three parameters, the temperature dependence is dominant in the lateral growth constant λ . Indeed, it has been shown experimentally for SiO_2 films^{12,13} that temperature changes result in different growth exponents β , and it was established explicitly that the two temperatures 611 and 723 K correspond to $\lambda=0.2$ and $\lambda=3$, respectively. Similarly, by using *in situ* real-time x-ray reflectivity measurements for ion-sputtered Pd(001),³⁹ it has been shown that the surface roughness w and the exponent β can be manipulated by changing the temperature. Here, an experimental temperature range from 306 to 440 K was found to lead to a large variation of the growth exponent β in the range from 0.5 to 0.1, and this was related to the prefactors in the extended Kuramoto-Sivashinsky model.⁴⁰ Hence, one can envisage implementing a time-delayed feedback loop and stabilizing desired growth exponents by suitable

adjustments of the temperature. In summary, this Brief Report proposes to apply novel concepts from control theory to a broad class of nonequilibrium growth models. The fundamentally different aspect is that the scaling exponents can be controlled, over a significant time span, by an *internal* feedback loop rather than an *external* manipulation of the underlying physical processes.

We have benefitted from helpful discussions with Uwe Täuber and Erwin Frey. B.S. wishes to thank the Sfb 296 and the ITP at TU Berlin for their hospitality. This work was supported in part by the Deutsche Forschungsgemeinschaft through Sfb 296, and by the U.S. National Science Foundation through DMR-0414122.

*FAX: +49-(0)30-314-21130; block@itp.physik.tu-berlin.de

¹*Handbook of Chaos Control*, edited by H.-G. Schuster (Wiley-VCH, Berlin, 1999).

²H. Nijmeijer and A. Schaft, *Nonlinear Dynamical Control Systems* (Springer, New York, 1996).

³K. Pyragas, Phys. Lett. A **170**, 421 (1992).

⁴E. Schöll, *Nonlinear Spatio-Temporal Dynamics and Chaos in Semiconductors* (Cambridge University Press, Cambridge, 2001).

⁵E. Schöll, Ann. Phys. **13**, 403 (2004).

⁶G. Stegemann, A. G. Balanov, and E. Schöll, Phys. Rev. E **73**, 016203 (2006).

⁷S. Schikora, P. Hövel, H.-J. Wünsche, E. Schöll, and F. Henneberger, Phys. Rev. Lett. **97**, 213902 (2006).

⁸J. Krug and H. Spohn, in *Solids Far From Equilibrium: Growth, Morphology and Defects*, edited by C. Godreche (Cambridge University Press, Cambridge, 1991).

⁹A.-L. Barabási and H. E. Stanley, *Fractal Concepts in Surface Growth* (Cambridge University Press, Cambridge, 1995).

¹⁰J. Krug, Adv. Phys. **46**, 139 (1997).

¹¹M. Kardar, G. Parisi, and Y.-C. Zhang, Phys. Rev. Lett. **56**, 889 (1986).

¹²F. Ojeda, R. Cuerno, R. Salvarezza, and L. Vázquez, Phys. Rev. Lett. **84**, 3125 (2000).

¹³F. Ojeda, R. Cuerno, R. Salvarezza, F. Agulló-Rueda, and L. Vázquez, Phys. Rev. B **67**, 245416 (2003).

¹⁴M. A. Auger, L. Vázquez, R. Cuerno, M. Castro, M. Jergel, and O. Sánchez, Phys. Rev. B **73**, 045436 (2006).

¹⁵R. Surdeanu, R. J. Wijngaarden, E. Visser, J. M. Huijbregtse, J. H. Rector, B. Dam, and R. Griessen, Phys. Rev. Lett. **83**, 2054 (1999).

¹⁶D. Forster, D. R. Nelson, and M. J. Stephen, Phys. Rev. A **16**, 732 (1977).

¹⁷H. van Beijeren, R. Kutner, and H. Spohn, Phys. Rev. Lett. **54**, 2026 (1985).

¹⁸H. K. Janssen and B. Schmittmann, Z. Phys. B: Condens. Matter **63**, 517 (1986).

¹⁹B. Schmittmann and R. K. P. Zia, in *Statistical Mechanics of*

Driven Diffusive Systems, edited by C. Domb and J. L. Lebowitz, Phase Transitions and Critical Phenomena Vol. 17 (Academic, New York, 1995).

²⁰A. Brú, S. Albertos, J. A. Lopez García-Asenjo, and I. Brú, Phys. Rev. Lett. **92**, 238101 (2004).

²¹A. Brú, S. Albertos, J. L. Subiza, J. L. García-Asenjo, and I. Brú, Biophys. J. **85**, 2948 (2003).

²²A. Brú, J. M. Pastor, I. Fernaú, I. Brú, S. Melle, and C. Berenguer, Phys. Rev. Lett. **81**, 4008 (1998).

²³J. Maunukela, M. Myllys, J. Timonen, M. J. Alava, and T. Ala-Nissila, Physica A **266**, 372 (1999).

²⁴A. S. Balankin, O. M. Matamoros, M. E. Galvez, and A. A. Perez, Phys. Rev. E **69**, 036121 (2004).

²⁵F. Elsholz, E. Schöll, C. Scharfenorth, G. Seewald, H. J. Eichler, and A. Rosenfeld, J. Appl. Phys. **98**, 103516 (2005).

²⁶Z. W. Lai and S. D. Sarma, Phys. Rev. Lett. **66**, 2348 (1991).

²⁷T. Nattermann and L. H. Tang, Phys. Rev. A **45**, 7156 (1992).

²⁸J. Krug, M. Plischke, and M. Siegert, Phys. Rev. Lett. **70**, 3271 (1993).

²⁹S. Das Sarma, C. J. Lanczycki, R. Kotlyar, and S. V. Ghaisas, Phys. Rev. E **53**, 359 (1996).

³⁰M. Marsili, A. Maritan, F. Toigo, and J. R. Banavar, Europhys. Lett. **35**, 171 (1996).

³¹B. Schmittmann, G. Pruessner, and H.-K. Janssen, Phys. Rev. E **73**, 051603 (2006).

³²F. Family and T. Vicsek, J. Phys. A **18**, L75 (1985).

³³S. F. Edwards and D. R. Wilkinson, Proc. R. Soc. London, Ser. A **381**, 17 (1982).

³⁴C.-H. Lam and F. G. Shin, Phys. Rev. E **57**, 6506 (1998).

³⁵C.-H. Lam and F. G. Shin, Phys. Rev. E **58**, 5592 (1998).

³⁶M. J. Rost, D. A. Quist, and J. W. M. Frenken, Phys. Rev. Lett. **91**, 026101 (2003).

³⁷I. Ošt'ádal, P. Kočan, P. Sobotík, and J. Pudl, Phys. Rev. Lett. **95**, 146101 (2005).

³⁸T. C. Kim *et al.*, Phys. Rev. Lett. **92**, 246104 (2004).

³⁹T. C. Kim, M. H. Jo, Y. Kim, D. Y. Noh, B. Kahng, and J.-S. Kim, Phys. Rev. B **73**, 125425 (2006).

⁴⁰M. A. Makeev and A. L. Barabasi, Appl. Phys. Lett. **71**, 2800 (1997).